Integrated Terahertz Communication with Reflectors for 5G Small Cell Networks

Michael Taynnan Barros, Robert Mullins,
Sasitharan Balasubramaniam, *Senior Member*, IEEE

***Abstract*—As the cellular networks continue to progress between generations, the expectations of 5G systems are planned towards high capacity communication links that can provide users access to numerous types of applications (e.g., augmented reality, holographic multimedia streaming). The demand for higher bandwidth has led the research community to investigated unexplored frequency spectrum, such as the terahertz-band for 5G. However, this particular spectrum is strived with numerous challenges, which includes the need for Line-of-Sight (LoS) links as reflections will deflect the waves as well as molecular absorption that can affect the signal strength. This is further amplified when high Quality-of-Service (QoS) has to be maintained over infrastructure that supports mobility as users (or groups of users) migrate between locations, requiring frequent handover for roaming. In this paper, the concept of mirror-assisted wireless coverage is introduced, where smart antennas are utilised with dielectric mirrors that act as reflectors for the terahertz waves. The objective is to utilise information such as the user's location, and to direct the reflective beam towards the highest concentration of users. A multi-ray model is presented in order to develop the propagation models for both indoor and outdoor scenarios, in order to validate the proposed use of the reflectors. An office and a pedestrian walking scenarios are used for indoors and outdoors scenarios, respectively. The results from the simulation work shows an improvement with the usage of mirror-assisted wireless coverage, improving the overall capacity, received power, path loss and probability of line of sight.**

***Index Terms*—Terahertz communication, 5G, smart antennas, mirror-assisted wireless coverage, outdoor and indoor communications.**

I. Introduction

The evolutionary development of mobile networks has resulted in advanced technologies for both the handset as well as wireless access to the base stations. This development has provided users with unprecedented data rates enabling various types of rich multimedia services to be realized (e.g., high definition video conferencing). However, moving forward into the future, the expectations for higher data rates will increase, where this will largely be enforced from more advanced applications and services (e.g., *Self-driving cars*, *Augmented Reality Experience* and *Internet of Bio-Nano Things* [1], [2], [3], [4]). By 2020, the IP data handled by wireless networks is expected to exceed 500 exabytes [5], [6]. The next generation 5G networks, which is currently in the research and development stage, has laid out a set of requirements that was not fully realized by the Long-Term Evolution (LTE) technology, and these requirements include high data rate and capacity (10Gbps) while maintaining the end-user Quality of Service (QoS), energy-efficient and green communication systems, as well as flexible management of resources. The latter requirement is particularly of great interest to the mobile network operators, where the network management of 5G networks is moving towards decoupling the data and control plane [6]. This revolutionary change will be realized through Software-Defined Networking (SDN) as well as Network Function Virtualization (NFV) [7].

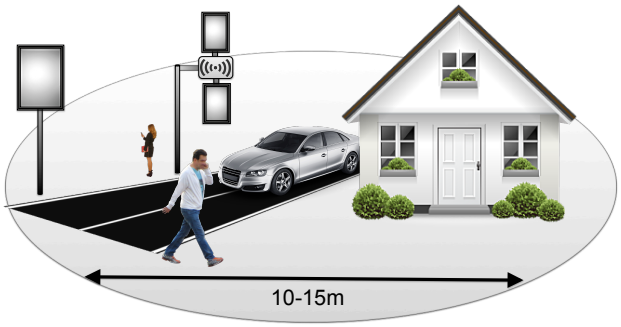

Fig. 1: Smart antennas for 5G small cells with terahertz-band communication. These antennas have *dielectric mirror* coupled to each antenna and assist by reflecting signals from neighbouring base stations. We term this coordination of reflectors as *mirror-assisted coverage*.

While new forms of software deployments are being planned for 5G systems, there is also a need to discover new wireless technologies between the handset and the base stations that is able to handle very high speed transmissions. One approach that has been investigated in recent years, is to push the carrier frequencies into the *Terahertz-band* in order to achieve data rate that is close to 10^{12}bps. Antennas communicating in this frequency range has been proposed for small cells with small coverage areas. These small cells, with a range between 10 - 15m, are able to maintain a decent level of signal quality for high end-to-end capacity in areas with high density of mobile users. Deploying these small cells that operate in parallel with the macro cells, also provides an opportunity to offload traffic in order to reduce the operation costs [8].

Nevertheless, terahertz-band communication has many challenges regarding the reliability of link stability due to 1) Non-line of sight connections (NLoS) that exist in the environment,

Michael Taynnan Barros and Robert Mullins are with the Telecommunication Software & Systems Group (TSSG), Waterford Institute of Technology (WIT), Ireland.

Sasitharan Balasubramaniam is with the Nano Communications Center (NCC), Department of Electronics and Communication Engineering at Tampere University of Technology (TUT), Finland.

E-mail: mbarros@tssg.org, sasi.bala@tut.fi, rmullins@tssg.org

2) molecular absorptions due to the weather and 3) frequency response due to Doppler effect. When signals are transmitted in the terahertz-band, the data rate drops considerably for NLoS links due to reflection and/or scattering losses on rough surfaces [9], [10]. Molecular absorption also negatively impacts the communication channel, where the water vapour are known to attenuate the signal. Finally, multi-path propagation and Doppler effect are known problems for outdoors scenarios, which have not been properly studied in the terahertz-band communication, and are considered highly challenging to the communication system performance [11], [12].

In order to address the issues addressed above, this paper proposes smart antennas that are designed to provide mirror-assisted coverage for 5G small cell utilizing terahertz-band communication. Fig. 1 illustrates our proposed antennas for both indoor and outdoor environments. Each of the antenna contain a number of moveable dielectric mirrors that are able to adaptively reflect and direct the beams from other antennas, leading to increased signal power and gain in specific locations.

In order to provide substantial insights about the benefits of the proposed approach, a multi-ray channel model for wideband terahertz-band communication is presented. The model accounts for spreading, molecular absorption, reflection, and scattering losses. Two scenarios are studied in order to investigate both indoor and outdoor areas. For indoors communication, an office scenario is modelled, while for the outdoors, a walking pedestrian model is developed. For each scenario, blockage models have been obtained to study both medium and high blockage densities. For each of these scenarios, four metrics will be evaluated and this includes path loss, received power, capacity and probability of line of sight.

Our contribution can be summarized as follows:

- **Mirror-assisted coverage for small cells with dielectric mirrors.** A new antenna architecture coupled to dielectric mirrors is presented for terahertz signal propagation improvements. The coverage power can be redirected and/or concentrated to specific areas through coordinated rotation of the mirrors. The benefit of this approach is to be able to beam and concentrate signal strength towards locations with high density of mobile handsets.
- **Capacity, path-loss and received power analysis for mirror-assisted 5G small cells.** The analysis presented in this paper show a remarkable benefit for small cell deployment that can exploit the terahertz-band to improve the network capacity. This is important development towards the realisation of ultra-dense wireless 5G networks that can provide high data rate capacity for mobile users.
- **Probability of line of sight has been improved with mirror coordination.** Through the usage of simple mirror coordination, the probability of line of sight has been improved and the increase of received power has been achieve with the concept of *virtual line of sight*. The analysis presented in the paper goes through various locations within a confined space, and how the performance can be improved through coordination of mirrors.

The rest of the paper is organized as follows: §II presents the terahertz-band communication technology and its model, §III presents the method in using smart antennas using adaptive beamforming and reflection properties, §IV presents the analysis for quantifying our contribution and lastly in §V the conclusion of the paper is presented.

II. Terahertz-band Communication

The most cited technology for providing high date rate satisfying 5G demands is terahertz-band communication [11]. Communicating at this band can lead to transmission of up to 10^{12}bps, providing reliable 5G-based applications that require high data rate. The frequencies between 100 GHz to 10 THz can provide ultra-broadband spectrum usage as well as being suitable for high spectrum efficiency. While these spectrum band seems appealing, it is not fully developed for communications, and in particular for small cells. Currently, researchers are concentrating their efforts on accurate communication models and their validation before this technology could be deployed. Proposed models such as [13], [14], [15], present an in-depth study into the different peculiarities that are uniquely found in the terahertz-band. These models, however, have scalability issues as well as other limitations that include multiple propagation effects. Works like [16], [17], [18] have proposed more complete and advanced models using ray tracing techniques for the band ($0.06-1$THz). In the following, a terahertz signal propagation model is presented. It will serve as the base for validating the proposed approach of mirror-assisted antennas with reflectors for 5G terahertz-band communication in small cells.

A. Terahertz Signal Model

Aiming to present an accurate multi-ray propagation model for the $0.06 - 10$THz band communication, the ray tracing method incorporates principles from optics. This is based on the characterization of electromagnetic waves in the studied frequency range [16], and is based on the works of [12], [16], [17], [9], [9], [18].

The multi-ray model considers propagation effects, including: *spreading* ($\Psi(f,r)$), *molecular absorption* ($\beta(f,r)$), *reflection* ($\Gamma(f,r)$) and *scattering* ($\zeta(f,r)$), in which f is frequency and r is distance. In the following, each of these effects are formulated.

1) Spreading: Spreading is the effect of electromagnetic signal propagation for a LoS configuration and, in the case of the terahertz-band, can be obtained in the following way [12]:

$$\Psi(f,r) = \left(\frac{c}{4\pi f r}\right)^2, \tag{1}$$

where c is the speed of light in vacuum. Particularly, the effect of spreading in the terahertz-band can be quite small in terms of gain, and can be an issue for long-range communication links.

2) Molecular Absorption: The molecular absorption loss impacts considerably on the terahertz signals and must be considered. This can be characterized as [12]:

$$k(f) = \sum_g \frac{p}{p_0}\frac{T_0}{T}\sigma^g(f), \tag{2}$$

where p is the system pressure, p_0 is the reference pressure, T_0 is the standard temperature, T is the system temperature and $\sigma^g(f)$ is the absorption cross-section. According to [12], the major contributor to the total absorption is water vapor and this is the only gas considered in this study.

The radiative transfer theory is used for quantification of the molecular absorption loss depending on frequency and distance. For this, the Beer-Lambert law is considered [12], and represented as

$$\beta(f,r) = e^{-\frac{1}{2}k(f)r}. \tag{3}$$

3) Reflection: The Kirchhoff theory is used for calculating the reflection loss of terahertz waves. The Fresnel reflection coefficient and the Rayleigh roughness factor are used in this analysis. The Fresnel reflection coefficient can be obtained from [9]:

$$R(f) = \frac{\cos(\theta_i) - n_t\sqrt{1-(\frac{1}{n_t}\sin(\theta_i))^2}}{\cos(\theta_i) + n_t\sqrt{1-(\frac{1}{n_t}\sin(\theta_i))^2}}, \tag{4}$$

in which θ_i is the angle of the incident wave and n_t is the refractive index of a medium.

The Rayleigh roughness factor can be defined as [9]:

$$\rho(f) = e^{-\frac{G(f)}{2}}, \tag{5}$$

with

$$G(f) = \left(\frac{4\pi\omega\cos(\theta_i)}{c}\right)^2, \tag{6}$$

where ω is the standard deviation of the surface roughness and c is the free space wavelength of the incident wave.

Thus, the reflection loss can be written as [16]:

$$\Gamma(f,r) = \sum_n \Psi(f,r) \times \beta(f,r) \times R(f) \times \rho(f), \tag{7}$$

in which n is the number of rays.

4) Scattering: Scattering affects terahertz signals based on the roughness level of the surface that it reflects itself from. This is considered critical to the communication link and must also be taken into account.

First, we consider the Beckham-Kirchhoff theory for obtaining the scattering coefficient and its approximation [16], which is represented as:

$$S(f) = -e^{\frac{-2\cos(\theta_1)}{\sqrt{n_t^2-1}}} \times \sqrt{\frac{1}{1+g+\frac{g^2}{2}+\frac{g^3}{6}}} \times \sqrt{p_0 + \frac{\pi\cos(\theta_1)}{100}(ge^{v_s} + \frac{g^2}{4}e^{\frac{-v_s}{2}})} \tag{8}$$

in which, the values of p_0, g, v_s and θ_1 can be found in [19].

Thus, the scattering loss can be obtained considering spreading, molecular absorption, the Rayleigh roughness factor and the scattering coefficient of n rays, and is represented as:

$$\zeta(f,r) = \sum_n \Psi(f,r) \times \beta(f,r) \times R(f) \times S(f). \tag{9}$$

B. Path-loss Model

A path-loss model can be obtained upon adding the attenuation loss of each signal propagation effect (spreading (Ψ), molecular absorption (β), reflection (Γ) and scattering (ζ)) in *dB*, and this is represented as:

$$\alpha(f,r) = 10\times\log_{10}(\Psi(f,r)) + 10\times\log_{10}(\beta(f,r)) + 10\times\log_{10}(\Gamma(f,r)) + 10\times\log_{10}(\zeta(f,r)) \tag{10}$$

C. Received Power Model

Link budget analysis is used to model received power in the terahertz-band communication for 5G systems. This technique is in accordance to previous studies for millimeter-wave communication and also terahertz communication [10]. The following formula is used:

$$R_{px} = P_{tx} + G_{tx} + G_{rx} - \alpha(f,r) - \gamma, \tag{11}$$

where R_{px} is the received power, P_{tx} is the transmission power, G_{tx} is the antenna gain in the transmitter, G_{rx} is the antenna gain in the receiver and γ is the loss resulting from shadowing.

For an in-depth analysis for quantifying the contribution of the paper, the received power model is separated for both indoors and outdoors scenarios. They are presented in the following:

1) Indoors: The indoor scenario is characterized by an area of 5 x 5m, resulting in a realistic office setting under room temperature. Parameter values from [10] were used, which considers P_{tx} = 1dBm with $7.4dB$ conversion loss, G_{tx} and G_{rx} are equal to 30dBi. However, the receiver has a conversion gain of 8dB with a noise figure of 7.5dB and $\gamma = -74$dBm. This results in

$$R_{pi} = 127.7 - \alpha(f,r). \tag{12}$$

2) Outdoors: For the outdoor scenario, an area of 20 x 20m is used to simulate a moving pedestrian. Signal reflection and scattering is found in the environment as they are reflected from building walls as well as other objects in the environments (e.g. trees, benches) (in this scenario we consider a pedestrian walking along a path in the city centre that is lined with buildings). Parameters values from [24], [25], [26], [27] were used, which considers P_{tx} = 2dBm, G_{tx} and G_{rx} are equal to 21dBi. The receiver has a conversion gain of 8dB with a noise figure of 7.5dB and $\gamma = -50$dBm. This results in

$$R_{pi} = 141.7 - \alpha(f,r). \tag{13}$$

TABLE I: Probability of line of sigh models obtained from [20], [21], [22], [23]

	Medium Blockage Density	High Blockage Density
Indoor	$plos(d) = \begin{cases} 1 & \text{if } d <= 1.2 \\ \exp -\frac{d-1.2}{4.7} & \text{if } 1.2 < d \leq 6.5 \\ \exp -\frac{d-6.5}{32.6} * 0.32 & \text{if } d > 6.5 \end{cases}$	$plos(d) = \begin{cases} 1 & \text{if } d <= 1.2 \\ \exp -\frac{d-1.2}{2.35} & \text{if } 1.2 < d \leq 6.5 \\ \exp -\frac{d-6.5}{16.3} * 0.32 & \text{if } d > 6.5 \end{cases}$
Outdoor	$plos(d) = \begin{cases} 1 & \text{if } d <= 1.2 \\ \exp -\frac{d-1.2}{40} & \text{if } 1.2 < d \leq 6.5 \\ \exp -\frac{d-6.5}{82.5} & \text{if } d > 6.5 \end{cases}$	$plos(d) = \begin{cases} 1 & \text{if } d <= 1.2 \\ \exp -\frac{d-1.2}{80} & \text{if } 1.2 < d \leq 6.5 \\ \exp -\frac{d-6.5}{165} & \text{if } d > 6.5 \end{cases}$

D. Blockage model

Using simple regression model analysis obtained from [20], [21], [22], [23], the blockage analysis is presented in the following through the calculation of the *probability of line of sight*. The indoor scenario is modelled according to an office-like environment which includes: open-plan office with cubical area, closed-plan office with corridor and meeting room, and also a hybrid-plan office with both open and closed areas. On the other hand, the outdoors scenario is accountable for buildings in a urban scenario, which is based on the 3GPP 3D model. All models, including both medium and high blockage densities, are found in Table I.

E. Capacity model

In order to evaluate the capacity based on the presented propagation model, we use a wideband window model dividing the terahertz-band into sub-band channels. This is necessary due to the inherent frequency-selective characteristic of the terahertz channel. A number of i sub-band channels is selected with a Δf width each. The resulting channel capacity is represented as:

$$C(d) = \sum_i \Delta f \log_2 \left[1 + \frac{\alpha(f,r)^{-1} S_i}{N_0} \right], \qquad (14)$$

in which S_i is the transmitting power p.s.d. and N_0 is the noise p.s.d. and is considered flat for all the sub-bands [28]. More investigation into the noise in the terahertz-band is still required [11].

III. Smart Antennas for 5G Terahertz-band Communication

Based on the numerous issues that are imposed from communicating in the terahertz-band, the usage of smart antennas and mirrors for enabling *mirror-assisted wireless coverage* is proposed in this paper. Mirror-assisted wireless coverage can reflect rays that beam to a concentrated area, where the total signal reception will have higher strength. The mirror-assisted wireless coverage for terahertz-band communication can be beneficial for the three issues discussed in the introduction (NLoS connections, molecular absorption and node mobility.) Due to the refractive index of mirrors, NLoS signals that are reflected by them are not as affected by rough surfaces. Wireless signal coverage can also be redirected adaptively to areas with lower molecular absorption loss. Lastly, mirror-assisted wireless coverage can be beneficial for locations that have different density of end-user handsets, or also adaptively changing the critical coverage area as the nodes migrate. In the following, deeper investigation will be explored for smart antennas structure, terahertz signal reflection, antenna beam adaptation and, finally, mirror-assisted wireless coverage.

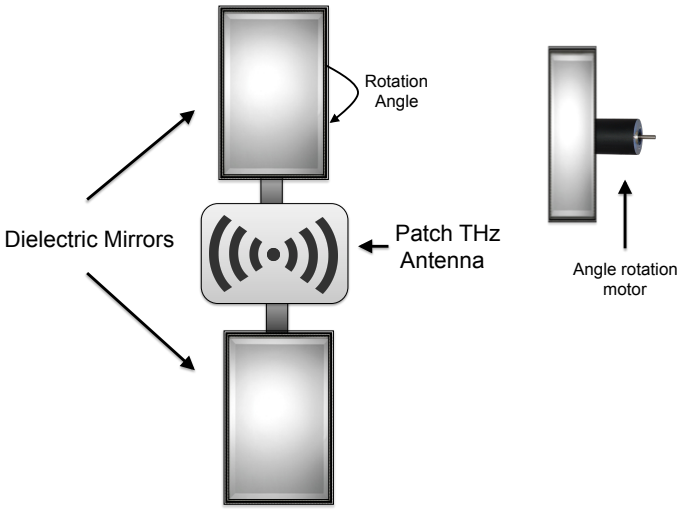

Fig. 2: Structure of the Smart Antennas for terahertz-band communication in 5G small cells. Dielectric mirrors are coupled to the antenna structure. These mirrors allow reflection of terahertz waves. Also they are able to change their angle to adaptively change the antennas' focus.

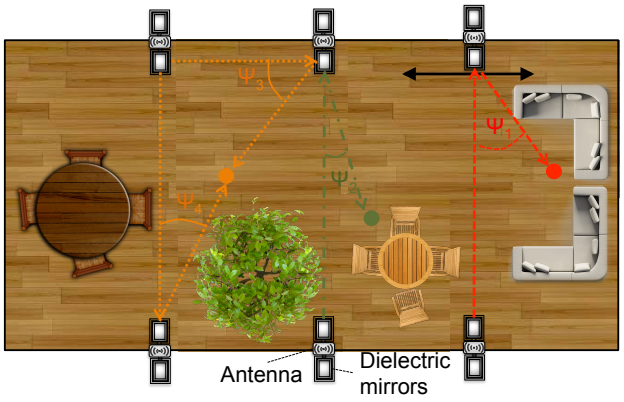

Fig. 3: Demonstration of mirror angle adaptation allowing redirection of rays to a particular spot, enabling a critical coverage area.

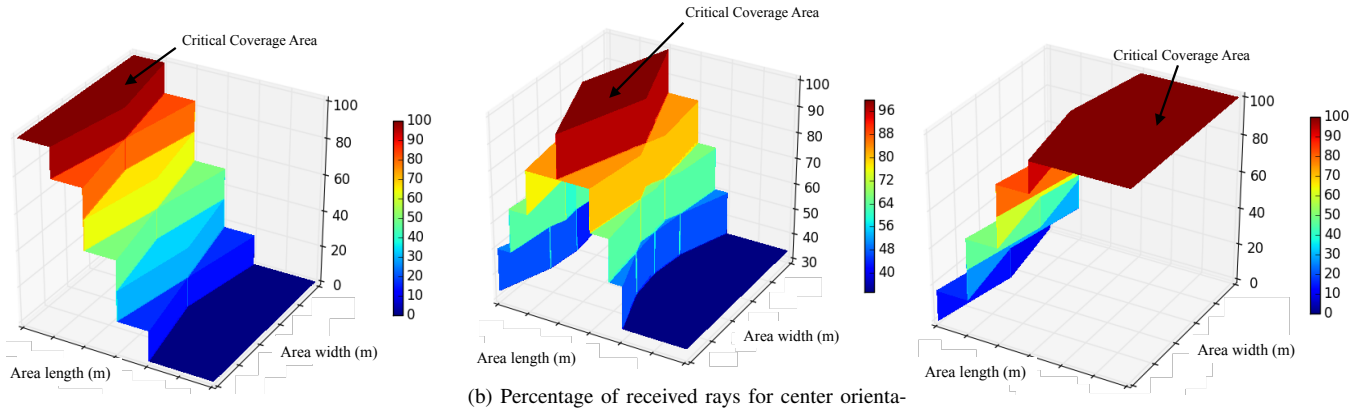

(a) Percentage of received rays for left orientation

(b) Percentage of received rays for center orientation

(c) Percentage of received rays for right orientation

Fig. 4: Virtual line of sight following left, center and right orientation according to the intended positioning of the critical coverage areas.

A. Smart Antennas Structure

The full structure of the proposed smart antennas is shown in Fig. 2. The dielectric mirrors are coupled to the antenna structure in order to provide reflections of terahertz signals with minimum attenuation possible. Although they are attached to the antenna itself, it is used to reflect the signals from the neighbouring base stations, rather that its own. It is envisioned that the dielectric mirrors have motors attached to their interior surface, which will allow them to rotate and adaptively change their configuration. This in turn, will satisfy the requirements of having a decoupled network control plane, as part of the vision of 5G. In order to satisfy this, knowledge with regards to the transmitter and receiver positions are required, and this information can be provided from the control plane. In the case of multiple mirrors usage, these can cooperatively change the focus to a specific location, named *critical coverage area*. Fig. 3 illustrates the coordination of mirror angles directing rays to a critical coverage area. In that location, the signal strength will be aggregated to give priority to specific locations of the environment that may consist of high density of nodes.

B. Reflecting Terahertz Signal

The mirrors are composed of multiple thin layers of dielectric material with the possibility of optical coating that enables the selection of specific wavelengths that can be reflected. These mirrors are cheap and reflection of terahertz-band waves is completely viable [29]. Piesiewicz et al [30] have proposed a scenario using dielectric mirrors, in which the interior of a room would be totally covered to allow reflection. Even though the benefits of such approach is remarkable, the impracticability of requiring walls covered with dielectric mirrors reduces the attractiveness of the proposed technology, and will lead to high costs.

For reflecting NLoS signals, mirrors should have a broad range of incident angles. One approach to satisfying this requirement is the usage of omnidirectional mirrors [31]. However, for perfectly reflecting signals between a transmitter and a receiver, the beams of the antennas should be synchronized, in which beams should be pointing to each other or the mirrors. In the case of an obstacle, the reflection through mirror creates a *virtual line of sight*. For that, the following is required: 1) the mirrors need to adaptively change to compensate the rays' incident angle, 2) the mirrors should know the transmitter and receiver location and adaptively change their angles to provide a virtual visibility between them, 3) antenna beams of both the transmitter and receiver should be pointing towards the mirror. These challenges require proper knowledge of the network infrastructure and the current status of the users within the area.

C. Antenna Beam Adaptation

We assume a linear smart antenna array with N nodes and total gain of GT_x for the transmitter and GR_x for the receiver [32]. We also assume perfect conditions for beamforming, beamsteering and beamwidth for the usage of the virtual line of sight concept, that can be further explained in the following:

1) *Beamforming*: Adaptive antenna beamforming is an existing technique for providing directional signals without having to move the transmitters and receivers. In the context of smart antennas with dielectric mirrors, this is needed to create a *virtual line of sight*, as described earlier. While reflecting terahertz rays, the antenna beamforming will point the direction towards dielectric mirrors which will reflect the signals with minimum attenuation.
2) *Beamsteering*: The smart antennas have to perform beamsteering for synchronization of the main lobe with the mirror, which is fundamental for realizing the virtual line of sight. Let Ψ_i be the angle between the upper (bottom) side of the area and the smart antenna boresight (see Fig. 3). We assume that Ψ_i takes values in $G = [-\frac{\pi}{2}, \frac{\pi}{2}]$. As such, the main lobe of each smart antenna is always directed towards the area of transmission.
3) *Beamwidth*: Beamwidth is another smart antenna characteristic that has fundamental importance on the virtual line of sight. The patch THz antenna can control the beamwidth adaptively [33], allowing the synchronization of the T_x antenna $3dB$ zone with the mirror.

D. Mirror-assisted Wireless Coverage

Combining the adaptive antenna beamforming with dielectric mirrors can achieve mirror-assisted wireless coverage. The adaptive in this case is when the beams are directed towards the highest number of users by only turning the angles of the dielectric mirrors. In this subsection, graphical visualization of the virtual line of sight is illustrated in Fig 4. A fixed area is assumed with six mirrors placed on the two opposite walls. Three situations are shown, where the critical coverage area is intended to be 1) on the left, 2) in the center and 3) on the right side of the area. A uniform distribution is assumed for the reflected rays from all the mirrors. The beamform of the antenna is very important for an optimal signal reception, however, this characteristic is neglected in this analysis since the intention is to only show the percentage of reflected rays. *The aim here is to show that the maximum percentage of the reflected rays for the virtual line of sight is obtained inside the critical coverage area.*

IV. Analysis

In order to evaluate the proposed smart antenna approach (*mirror-assisted coverage*), and theoretically compare to the conventional terahertz-band performance (*static coverage*), an extensive analysis is developed based on the ray tracing algorithm. The analysis considers path loss, received power, capacity and probability of line of sight for both indoor and outdoor communication scenarios with also medium and high blockage. In the following subsection, a description of the ray tracing algorithm is first described followed by the results of the analysis.

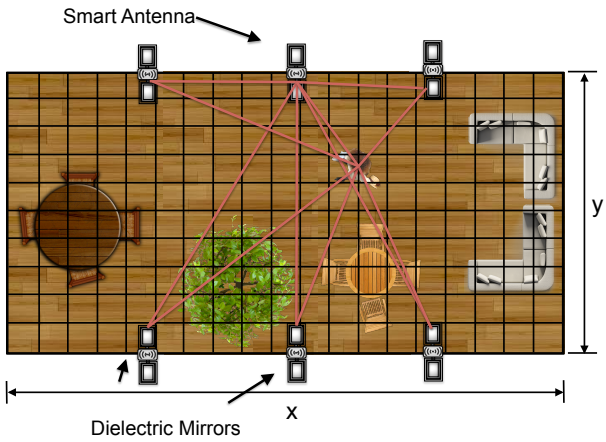

Fig. 5: Scenario used for distance analysis. The antenna is placed in the central-top position of the area. This scenario is used for both the adaptive and mirror-assisted coverage.

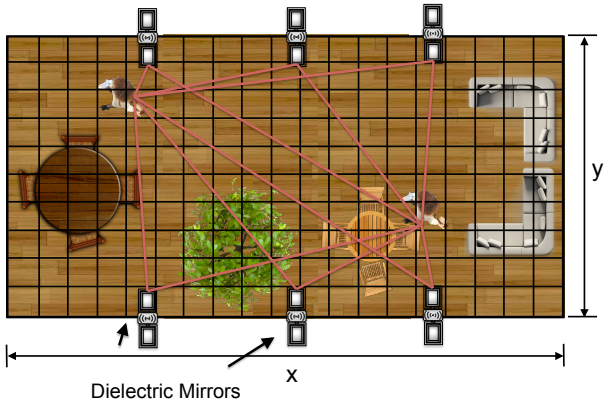

Fig. 6: Scenario used for frequency analysis. The transmitter (T_x) is place in the center of the area and the receiver (R_x) a few meters away.

A. Ray Tracing Simulation

A ray tracing algorithm was developed for the insertion of the propagation loss model resulting from spreading, molecular absorption, scattering and reflection effects in the terahertz-band communication. The developed technique was based on the works from [27], [16], [10]. For an area with dimensions of x and y meters containing $n \times m$ number of tiles, the ray tracing algorithm proceeds with the following four steps: 1) reflection/scattering points are determined, as well as mirror placements; 2) placement of the transmitter (T_x); 3) computation of the incident angles based on the defined rays; 4) computation of the capacity, received power, path loss and probability of line of sight according to the modelling presented in Section II for each tile of the area.

The dielectric mirrors are modeled based on their refractive properties. According to [30], the refractive index (n_t) is 3.418. These mirrors consist of four $63\mu m$ thick layers of high-resistant silicon. This property can easily be added to the Fresnel reflection coefficient in Eq. 4. Based on this the rays

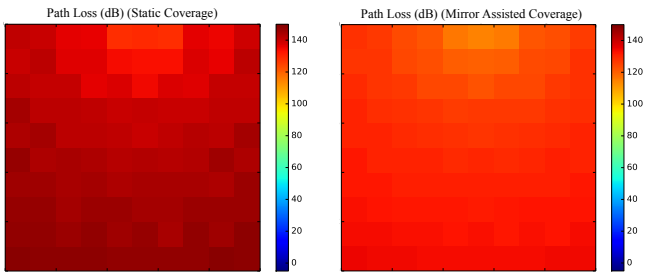

Fig. 7: Heatmap of path loss of a 10 x 10 m area with 10 x 10 tiles. The frequency used is 0.3 THz. a) static coverage and b) mirror-assisted coverage.

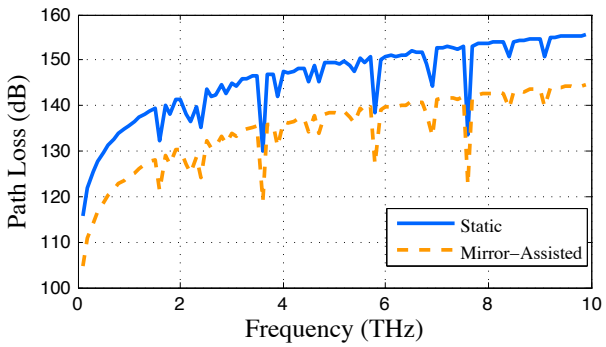

Fig. 8: Path Loss as function of frequency (Thz) for a 10 x 10 m area with 10 x 10 tiles. The distance between T_x and R_x is 1m.

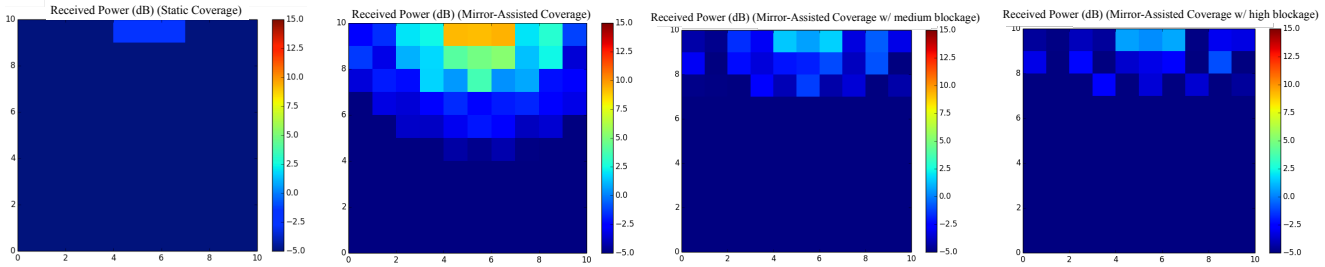

(a) (b) (c) (d)

Fig. 9: Heatmap of received power for indoor communication scenario of a 5 x 5 m area with 5 x 5 tiles, and the frequency used is 0.3THz. Four scenarios are considered, which includes a) static coverage, b) mirror-assisted coverage with no blockage c) mirror-assisted with medium density blockage, and d) mirror-assisted with high density blockage.

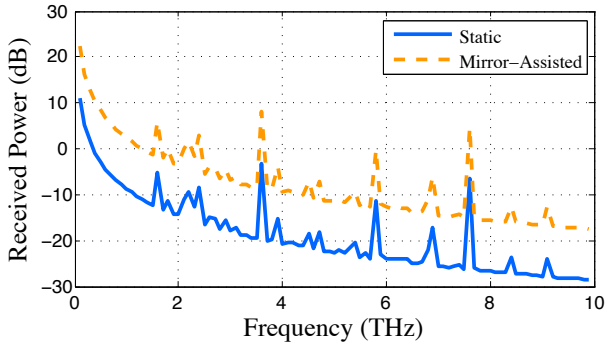

Fig. 10: Indoor communication received power as a function of frequency (Thz) for a 5 x 5 m area with 5 x 5 tiles. The distance between the transmitter and receiver is 1m.

that hit the mirrors are attenuated based on their refractive index.

Two approaches are compared, static and mirror-assisted coverage. In the first, the antennas are used with no antenna beam adaptation or mirrors. In the latter case, the antennas incorporate the beam adaptation and are able to point to the receiver direction utilising the dielectric mirrors for signal reflections.

For the distance analysis, the antenna are placed on the central-top position of the area as illustrated in Fig. 5. In the case of the frequency analysis, the transmitter (T_x) is placed in the center of the area and the receiver (R_x) a few meters away as illustrated in Fig. 5. For the frequency analysis the band range considered is divided into sub-bands.

B. Path Loss

The path loss, represented in (10), has a frequency-distance dependency that is explored in this subsection. The distance analysis of path loss is illustrated through heatmaps in Fig. 7. For each tile within the 10 x 10 m space, the mirror-assisted coverage will direct the mirrors to beam the rays towards that specific tile. Therefore, each tile has lower path loss intensity for the mirror-assisted coverage compared to the static. This is due to the rays that were previously attenuated based on the reflection and scattering of rough surfaces in the static coverage case are redirected through the dielectric mirrors compensating for lower total path loss in each tile.

This is also the same for frequency variation illustrated in Fig 8. Path loss increases with the frequency, and this is due to the molecular absorption loss. The distribution of the water vapor over frequency and distance is given by (3). However, once again, the mirror-assisted case improves the path loss as the frequency is varied to the higher end of the terahertz spectrum.

C. Indoor Environment

An office scenario is explored for the indoor environment, where the room area is 5 x 5 m with standard temperature and pressure to maintain the proper level of water vapor. In this analysis we are keen to investigate the received power using the model in (12), and in particular the performance when the environment contains different quantities of objectives and blockages. For the case of objects placed in the room, the medium and high blockage are represented in Table I

Fig. 9 presents the results of the total power on each tile in the room, and is represented through heat maps. *The quantity of intensity on each tile shows that the received power has been increased when the mirrors are tilted at the right angle to direct the beams to right location.* Fig. 9 also illustrates the effects of medium and high blockage within the room, and how this affects the total power in each tile. As illustrated in Fig. 9 (c) the medium blockage is still able to recover a certain amount of power with the reflections from the mirrors, and this is performance is slightly decreased in the case of high blockage in Fig. 9 (d).

Fig. 10 presents the received power for both static and mirror-assisted coverage techniques as the frequencies are varied. *As expected, the results shows that the coordinated dielectric mirrors improves the received power even when the higher frequencies suffer from power degradation due to molecular absorption.*

D. Outdoor Environment

A mobile pedestrian scenario is explored for the outdoor environment analysis, where the area considered is 20 x 20 m space that contains a single road with a pedestrian walkway on the side. The side of the road also contains buildings on either sides where the antenna as well as the mirrors are placed. Medium and high densities of blockage are characterized by the number per area of buildings and/or vehicles that can

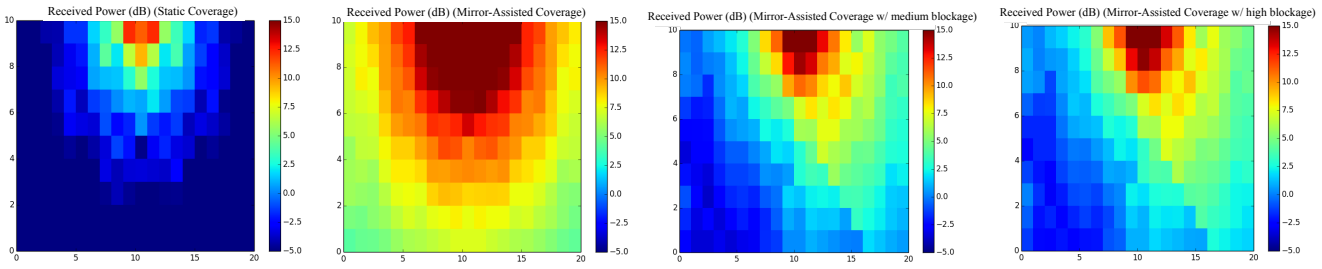

(a) (b) (c) (d)

Fig. 11: Heatmap of received power for outdoor communication scenario of a 20 x 20 m area with 10 x 10 tiles, where the transmitter frequency used is 0.3 THz. Four scenarios are considered, and this includes: a) static coverage, b) mirror-assisted coverage with no blockage, c) mirror-assisted coverage with medium density blockage, and d) mirror-assisted coverage with high density blockage.

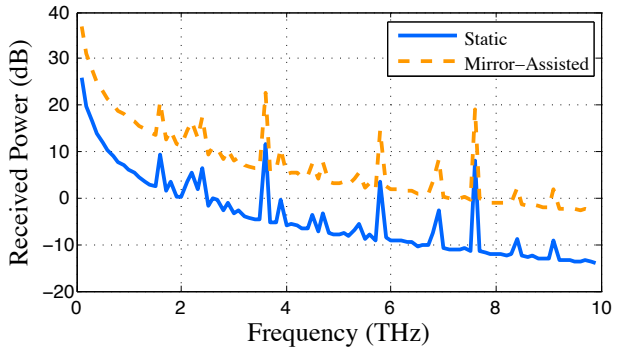

Fig. 12: Outdoor communication received power as function of frequency (Thz) for a 20 x 20 m area with 10 x 10 tiles. The distance between the transmitter and receiver is 2m.

completely block the line of sight connection. Similar to the indoor environment analysis, the analysis of the received power for the outdoor environment is represented by (13).

Fig. 11 presents the heatmap analysis of the received power comparison between static coverage, mirror-assisted coverage with no blockages, medium, and high density blockages. *Similar to the indoor case, the mirror-assisted coverage leads to higher power for each tile, and we can see that the signals are reflected through neighbouring mirrors to improve the performance for medium and high density blockages.* The blockage analysis is crucial for the outdoor case due to large objects (trees, lamp posts) and mobile objects (vehicles) within the environment that can lead to high amount of scattering when the signals are reflected. At the same time the outdoor case also has variations in the amount of molecular vapour that affects the signal absorption with 10% of water vapor. Therefore, the dynamic movements of the mirrors is very important to enable the signals to bounce around the high blockage areas to reach the receivers.

Fig. 12 shows the received power performance with respect to the variations in frequencies. As expected, the mirror-assisted coverage once again will reflect the signals around the blockages even the higher frequencies are more sensitive.

E. Impact on the Probability of Line of Sight

This section presents the model for the probability of line of sight based on the reflection from the mirrors. Consider an area of X and Y dimensions with n mirrors spread across the borders of the space. An uniform distribution is used to position the mirrors in the space with mirror $m = [m_x, m_y], m_x \in (1, X-1)$ and $m_y \in (0, Y)$. Consider now

$$M = \begin{bmatrix} m^{(1)} \\ m^{(2)} \\ \vdots \\ m^{(n)} \end{bmatrix} \tag{15}$$

as the matrix of mirrors and their positioning.

The probability of a single link line of sight for a transmitter ($T_x = [T_{xx}, T_{xy}]$), a receiver ($T_x = [T_{xx}, T_{xy}]$) and a single mirror ($m^{(i)}$) is represented as

$$P_{losM}(Tx, Rx, i) = \int_{m_x}^{m'_x} P_{los}(d(T_x, m^{(i)}))dx \times \int_{m_x}^{m'_x} P_{los}(d(m^{(i)}, R_x))dx \tag{16}$$

in which m'_x is the final position of the mirrors with length $L = m'_x - m_x$.

Therefore, the total probability of line of sight (TP_{los}) is achieve by

$$TP_{los} = (P_{los}(Tx, Rx) + \sum_{i=1}^{n} P_{losM}(Tx, Rx, i)) \times \frac{1}{n+1} \tag{17}$$

Fig. 13 presents the impact of the reflected signals from the mirrors on the probability of line of sight for both the indoor and outdoor environments. For each environment, both medium and high densities of blockages are considered. The probability is analysed as a function of both the communication distance (ranging from $0-9m$) and mirror size (ranging from $0-1m$ for indoor and $0-5m$ for outdoor environment). Square-shaped mirror are also considered. *The results showed that the probability of line of sight slightly vary as the communication distance increases, but increases significantly as the mirror size changes for the outdoor environment compared to indoor.* The size of mirrors are selected to be proportional to the size of the room as well as the power of emitted signals.

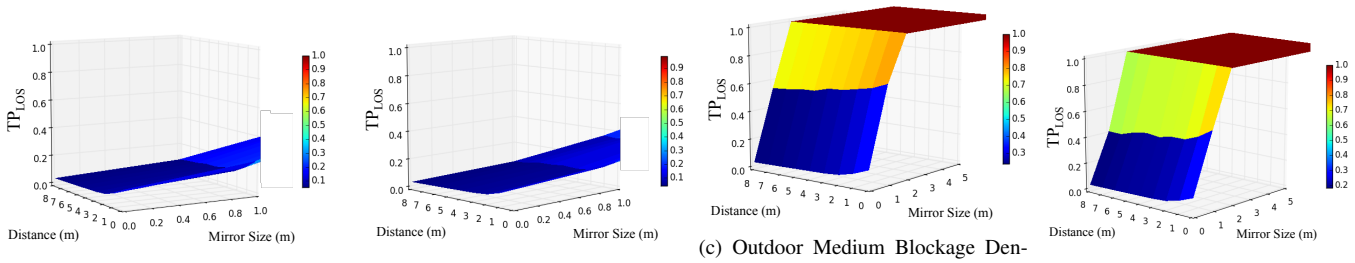

(a) Indoor Medium Blockage Density (b) Indoor High Blockage Density (c) Outdoor Medium Blockage Density (d) Outdoor High Blockage Density

Fig. 13: The impact of the terahertz signal reflection using mirrors on the probability of line of sight for both indoors and outdoors versus both medium and high blockage densities.The probability is analysed as a function of both communication distance (ranging from $0-9m$) and mirror size (ranging from $0-1m$ in indoors and $0-5m$ in outdoors.)

The mirror size does not have a major impact for the indoor case, but slightly increases as the size gets larger. However, in the the outdoor case, the power of the signal also meant more reflections in the environment making the mirrors leading to higher probability of line of sight. The size of the mirrors saturates at a particular point making the probability of line of sight saturate after the length size of $2m$. Also, for both indoor and outdoor the variations of the communication distances does not have a dramatical effect on the probability of line of sight.

F. Mirror Coordination and Blockage Analysis

Although in the power analysis for both indoor and outdoor increase for each tile within the environmental space, this assumes that each of the mirrors are coordinated to project the reflected signal towards specific locations. Therefore, an important requirement is to ensure that coordination of the mirrors are performed, which is an analysis conducted in this section. In Fig. 14 the relationship of mirror coordination (0%, 25%, 50%, 100%), low (0.3 THz), medium (2 THz) and high (4 THz) frequencies, as well as varying blockage densities (low, medium and high) on the received power for indoor environments is presented. The coordination refers to the ratio of mirrors that are synchronized reflect the signal to the right tile within the space. For each of the frequency value, the coordination of mirrors does not significantly improve the performance. Thus the increase in blockage densities does affect the performance even when there is increased mirror coordination. Lastly, the coordination does not affect the frequency of the signals dramatically.

Fig. 15 presents the same analysis for the case of the outdoor environment. Compared to the indoor case the outdoor environment has more positive effect from the mirror coordination, even when the quantity of blockage increases. The reason for the positive impact is due to the longer communication distances where the mirrors have an impact on longer range of directional angles, and therefore, can achieve better coverage areas. This helps to improve the received power performance in specific tile spots in the area.

G. Capacity Analysis

The capacity of a terahertz communication, represented by (14), has a frequency-distance dependency relationship which

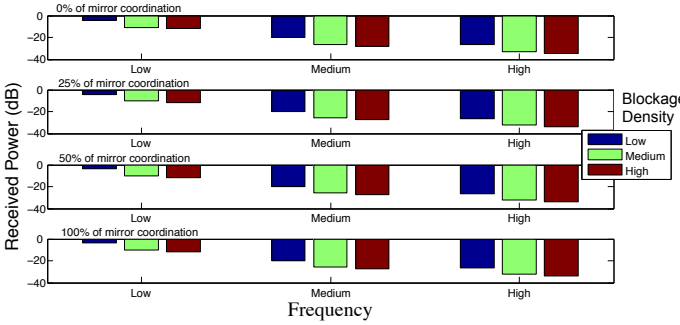

Fig. 14: The relationship of mirror coordination (0%, 25%, 50%, 100%), frequency (low (0.3 THz), medium (2 THz) and high(4 THz)) and blockage density (low, medium and high) on the received power in indoor environments.

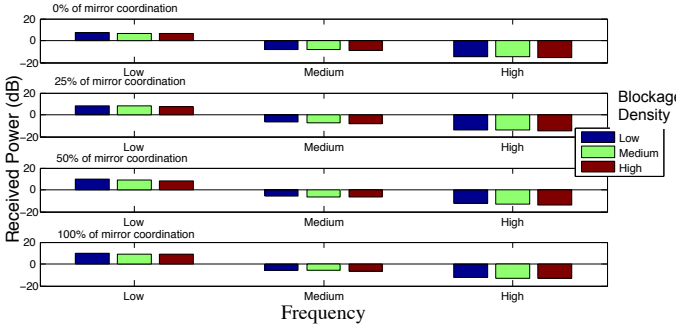

Fig. 15: The relationship of mirror coordination (0%, 25%, 50%, 100%), frequency (low (0.3 THz), medium (2 THz) and high(4 THz)) and blockage density (low, medium and high) on the received power in outdoor environments.

will be explored in this section. Both the power and noise p.s.d. are kept constant for our analysis, based on [12], [16], [28].

Capacity is improved using adaptive coverage over the distance increase. Terahertz-band communication performance is favourable for short-range distances, and decreases exponentially as the distance is increased. However, as illustrated in Fig. 16, the mirror-assisted coverage can improve the overall capacity by nearly 10 times compared to the static case.

Similar to the distance variation, the variations in the frequency also affects the capacity performance. The higher the frequency, the more unstable it is and gets affected by the quantity of molecular vapour within the air, leading to

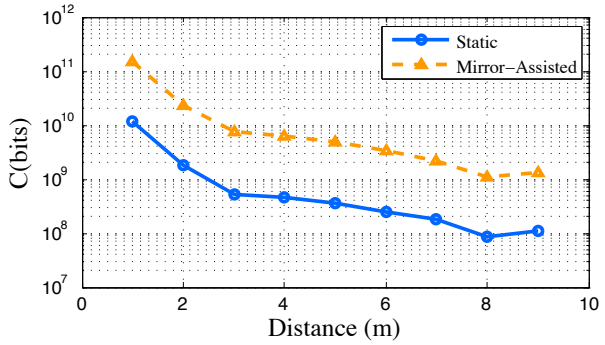

Fig. 16: Capacity as function of distance for a 10 x 10m area with 10 x 10 tiles. The frequency used is 0.3 THz and Δ_f is 10 THz.

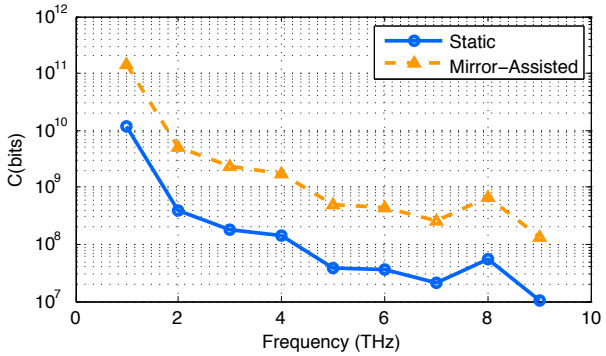

Fig. 17: Capacity as function of frequency (Thz) for a 5 x 5 m area with 5 x 5 tiles. Distance between transmitter and receiver is 1m and Δ_f is 1THz. Both static and adaptive coverage are studied.

reduced capacity. However, we can observe that around 8 THz there is a small increase in the capacity, and this is due to the frequency-selective characteristics of high terahertz frequency that are affected from molecular absorption. At this point, the mirror-assisted coverage will improve the performance by reflecting the signals round the regions with high quantity of water vapour.

Figs. 18 and 19 present the capacity results based on the relationship between varying the transmission power, density blockage, as well as coordination of mirrors for both the indoor and outdoors environments, respectively. For all the results, the transmission power has a linear dependency with capacity.
As observed in the results, increasing the transmission power is highly beneficial to the capacity, although this comes at a cost of higher power. Due to the density of blockage, *the capacity decreases for higher blockage density.*, but this performance increases due to the mirrors. The outdoors environment results in higher capacity due to the antenna gain for both the receiver as well as the transmitter. The presented results can be correlated with the analysis presented in Figs. 14 and 15.

V. Conclusion

The growth of IP data traffic that needs to be handled by future wireless networks (5G) is motivating the need for radical changes towards network flexibility. Future 5G requires high data rate transmission and few technologies are currently

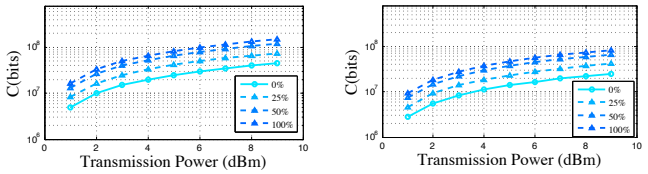

(a) Medium Blockage Density (b) High Blockage Density

Fig. 18: The relationship between transmission power, medium and high density blockages, coordination of mirrors and capacity for indoor environments.

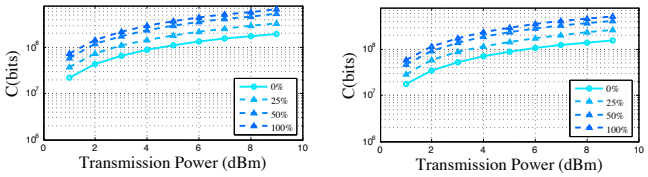

(a) Medium Blockage Density (b) High Blockage Density

Fig. 19: The relationship between transmission power, medium and high blockage, coordination of mirrors and capacity for outdoor environments.

being developed for that. Terahertz-band communication is the leading alternative to providing 5G with data rate up to 10^{12}. However, many challenges still inhibit terahertz-band communication, including: NLoS links, molecular absorption loss, and mobility. Based on this, the usage of smart antennas is suggested for terahertz-band communication. These antennas are capable of reflecting wireless signals, creating a virtual line of sight. Such technique mitigates losses from rough surfaces. However, beam synchronization between transmitter and receiver is required, and therefore, smart antennas must be used. Based on this, the concept of mirror-assisted wireless coverage was introduced.

To validate and provide insights of the mirror-assisted wireless coverage performance, a multi-ray propagation model was presented accounting for spreading, molecular absorption, reflection, and scattering losses. Indoor and outdoor communications were studied using the ray tracing simulation. Also, medium and high blockage densities were analysed with a blockage analysis for both indoors and outdoors. The system showed great improvement in the light of capacity, received power, path loss and line of sight. The presented approach has a tremendous potential to realizing 5G small cell networks using terahertz-band communication.

Acknowledgements

The work described in this paper is facilitated by the CogNet project (671625), which is funded under the European Commissions Horizon 2020 programme.

References

[1] J. G. Andrews, S. Buzzi, W. Choi, S. V. Hanly, A. Lozano, A. C. Soong, and J. C. Zhang, "What will 5g be?" *Selected Areas in Communications, IEEE Journal on*, vol. 32, no. 6, pp. 1065–1082, 2014.

[2] E. Larsson, O. Edfors, F. Tufvesson, and T. Marzetta, "Massive mimo for next generation wireless systems," *IEEE Communications Magazine*, vol. 52, no. 2, pp. 186–195, 2014.

[3] Y. Niu, Y. Li, D. Jin, L. Su, , and A. V. Vasilakos, "A survey of millimeter wave communications (mmwave) for 5g: opportunities and challenges," *Wireless Networks*, vol. 21, no. 8, pp. 2657–2676, 2015.
[4] I. F. Akyildiz, M. Pierobon, S. Balasubramaniam, and Y. Koucheryavy, "The internet of bio-nano things," *IEEE Communications Magazine*, vol. 53, no. 3, pp. 32–40, 2015.
[5] J. Andrews, "The seven ways hetnets are a paradigm shift," *IEEE Communications Magazine*, vol. 51, no. 3, pp. 136–144, 2013.
[6] J. G. Andrew, S. Buzzi, W. Choi, S. V. Hanly, A. Lozano, A. C. K. Soong, and J. C. Zhang, "What will 5g be?" *IEEE Journal Selected Areas in Communications*, vol. 32, no. 7, pp. 1065–1082, 2014.
[7] I. F. Akyildiz, S.-C. Lin, and P. Wang, "Wireless software-defined networks (w-sdns) and network function virtualization (nfv) for 5g cellular systems: An overview and qualitative evaluation," *Computer Networks*, vol. 93, Part 1, pp. 66 – 79, 2015.
[8] I. F. Akyildiz, E. Chavarria-Reyes, D. M. Gutierrez-Estevez, R. Balakrishnan, and J. R. Krier, "Enabling next generation small cells through femtorelays," *Physical Communication*, vol. 9, pp. 1 – 15, 2013.
[9] C. Jansen, R. Piesiewicz, D. Mittleman, T. Kurner, and M. Koch, "The impact of reflections from stratified building materials on the wave propagation in future indoor terahertz communication systems," *IEEE Transactions on Antennas and Propagation*, vol. 56, no. 5, pp. 1413–1419, 2008.
[10] C. Jansen, S. Priebe, C. Moller, M. Jacob, H. Dierke, M. Koch, and T. Kurner, "Diffuse scattering from rough surfaces in thz communication channels," *IEEE Transactions on Terahertz Science and Technology*, vol. 1, no. 2, pp. 462–472, 2011.
[11] I. F. Akyildiz, J. M. Jornet, and C. Han, "Teranets: ultra-broadband communication networks in the terahertz band," *IEEE Wireless Communications*, vol. 21, no. 4, pp. 130–135, 2014.
[12] J. M. Jornet and I. F. Akyildiz, "Channel modeling and capacity analysis for electromagnetic wireless nanonetworks in the terahertz band," *IEEE Transactions on Wireless Communications*, vol. 10, no. 10, pp. 3211–3221, 2011.
[13] S. Priebe, M. Kannicht, M. Jacob, and T. Krner, "Ultra broadband indoor channel measurements and calibrated ray tracing propagation modeling at thz frequencies," *Journal of Communications and Networks*, vol. 15, no. 6, pp. 547–558, 2013.
[14] H. J. Song, K. Ajito, A. Wakatsuki, Y. Muramoto, N. Kukutsu, Y. Kado, and T. Nagatsuma, "Terahertz wireless communication link at 300 ghz," in *IEEE Topical Meeting on Microwave Photonics (MWP)*, 2010, pp. 42–45.
[15] T. Krner and S. Priebe, "Towards thz communications-status in research, standardization and regulation," *Jounal of Infrared, Milimeter and Terahertz Waves*, vol. 35, no. 1, pp. 547–558, 2014.
[16] C. Han, A. O. Bicen, and I. F. Akyildiz, "Multi-ray channel modeling and wideband characterization for wireless communications in the terahertz band," *IEEE Transactions on Wireless Communications*, vol. 14, no. 5, pp. 2402–2412, 2015.
[17] ——, "Multi-wideband waveform design for distance-adaptive wireless communications in the terahertz band," *IEEE Transactions on Signal Processing*, vol. 64, no. 4, pp. 910–922, 2016.
[18] S. Priebe and T. Kurner, "Stochastic modeling of thz indoor radio channels," *IEEE Transactions on Wireless Communications*, vol. 12, no. 9, pp. 4445–4455, 2013.
[19] J. Harvey, A. Krywonos, and C. L. Vernold, "Modified beckmann-kirchhoff scattering model for rough surfaces with large incident and scattering angles," *Optical Engineering*, vol. 46, no. 7, p. 078002, 2007.
[20] K. Haneda, J. Zhang, L. Tan, G. Liu, Y. Zheng, H. Asplund, J. Li, Y. Wang, D. Steer, C. Li, T. Balercia, S. Lee, Y. Kim, A. Ghosh, T. Thomas, T. Nakamura, Y. Kakishima, T. Imai, H. Papadopoulos, T. S. Rappaport, G. R. MacCartney, M. K. Samimi, S. Sun, O. Koymen, S. Hur, J. Park, C. Zhang, E. Mellios, A. F. Molisch, S. S. Ghassamzadeh, and A. Ghosh, "5g 3gpp-like channel models for outdoor urban microcellular and macrocellular environments," in *2016 IEEE 83rd Vehicular Technology Conference (VTC Spring)*, May 2016, pp. 1–7.
[21] K. Haneda, L. Tian, H. Asplund, J. Li, Y. Wang, D. Steer, C. Li, T. Balercia, S. Lee, Y. Kim, A. Ghosh, T. Thomas, T. Nakamurai, Y. Kakishima, T. Imai, H. Papadopoulas, T. S. Rappaport, G. R. MacCartney, M. K. Samimi, S. Sun, O. Koymen, S. Hur, J. Park, J. Zhang, E. Mellios, A. F. Molisch, S. S. Ghassamzadeh, and A. Ghosh, "Indoor 5g 3gpp-like channel models for office and shopping mall environments," in *2016 IEEE International Conference on Communications Workshops (ICC)*, May 2016, pp. 694–699.
[22] S. Sun, T. A. Thomas, T. S. Rappaport, H. Nguyen, I. Z. Kovacs, and I. Rodriguez, "Path loss, shadow fading, and line-of-sight probability models for 5g urban macro-cellular scenarios," in *2015 IEEE Globecom Workshops*, Dec 2015, pp. 1–7.
[23] T. S. Rappaport, F. Gutierrez, E. Ben-Dor, J. N. Murdock, Y. Qiao, and J. I. Tamir, "Broadband millimeter-wave propagation measurements and models using adaptive-beam antennas for outdoor urban cellular communications," *IEEE Transactions on Antennas and Propagation*, vol. 61, no. 4, pp. 1850–1859, April 2013.
[24] T. Abbas, J. Nuckelt, T. Krner, T. Zemen, C. F. Mecklenbruker, and F. Tufvesson, "Simulation and measurement-based vehicle-to-vehicle channel characterization: Accuracy and constraint analysis," *IEEE Transactions on Antennas and Propagation*, vol. 63, no. 7, pp. 3208–3218, 2015.
[25] T. Gaugel, L. Reichardt, J. Mittag, T. Zwick, and H. Hartenstein, *High Performance Computing in Science and Engineering '11: Transactions of the High Performance Computing Center, Stuttgart (HLRS) 2011*, 2012, ch. Accurate Simulation of Wireless Vehicular Networks Based on Ray Tracing and Physical Layer Simulation, pp. 619–630.
[26] C. Sommer, D. Eckhoff, R. German, and F. Dressler, "A computationally inexpensive empirical model of ieee 802.11p radio shadowing in urban environments," in *Eighth International Conference on Wireless On-Demand Network Systems and Services (WONS)*, 2011, pp. 84–90.
[27] J. Nuckelt, T. Abbas, F. Tufvesson, C. Mecklenbrauker, L. Bernado, and T. Kurner, "Comparison of ray tracing and channel-sounder measurements for vehicular communications," in *IEEE 77th Vehicular Technology Conference (VTC Spring)*, 2013, pp. 1–5.
[28] T. Yilmaz and O. B. Akan, "On the use of low terahertz band for 5g indoor mobile networks," *Computers and Electrical Engineering*, vol. 48, pp. 164 – 173, 2015.
[29] D. Turchinovic, A. Kammoun, P. Knobloch, T. Dobberitn, and M. Koch, "Flexible all-plastic mirrors for the thz range," *Applied Physics A*, vol. 74, pp. 291–293, 2002.
[30] R. Piesiewicz, T. Kleine-Ostmann, N. Krumbholz, D. Mittleman, M. Koch, J. Schoebei, and T. Kurner, "Short-range ultra-broadband terahertz communications: Concepts and perspectives," *IEEE Antennas and Propagation Magazine*, vol. 49, no. 6, pp. 24–39, 2007.
[31] N. Krumbholz, K. Gerlach, F. Rutz, M. Roch, R. Piesiewicz, T. Kurner, and D. Mittleman, "Omnidirectional terahertz mirrors: A key element for future terahertz communication systems," *Applied Physics Letters*, vol. 88, p. 202905, 2006.
[32] I. Stevanovic, A. Skrivervik, and J. R. Mosig, "Smart antenna systems for mobile communications," Tech. Rep., 2003.
[33] H. Yu-xue, "Smart antenna technology," *Radio Communications Technology*, vol. 4, p. 010, 2006.

Michael Taynnan Barros was born in Campina Grande-PB, Brazil, 1990. He is currently an IRC Government of Ireland post-doc fellow associated with the Telecommunications Software and Systems Group (TSSG) and the Waterford Institute of Technology (WIT – Ireland). He is also working with EU-funded H2020 projects including, CogNet and Circle. Michael received his Ph.D. in Telecommunication Software at the Waterford Institute of Technology (WIT – Ireland-2016), M.Sc. degree in Computer Science at the Federal University of Campina Grande (UFCG – Brazil-2012) and B.Tech. degree in Telematics at the Federal Institute of Education, Science and Technology of Paraiba (IFPB – Brazil-2011). His experience concentrates on Vehicular AdHoc Networks, Cognitive Network Management, Molecular Communication and Terahertz Communication, publishing more than 35 papers in international journals and conferences. He is also a reviewer for many journals and participated as technical program committee and reviewer for various international conferences. Interests include Nanonetworks, Molecular Communication, Terahertz Communication and 5G for both connected-health and connected-cars.

Sasitharan Balasubramaniam Sasitharan Balasubramaniam (SM'14) received his Bachelor (Electrical and Electronic Engineering) and Ph.D. degrees from the University of Queensland in 1998 and 2005, respectively, and Masters (Computer and Communication Engineering) degree in 1999 from the Queensland University of Technology. He is currently a senior research fellow at the Nano Communication Centre, Department of Electronic and Communication Engineering, Tampere University of Technology, Finland. Previously, Sasitharan was a research fellow at the Telecommunication Software & Systems Group, Waterford Institute of Technology, Ireland, where he worked on a number of Science Foundation Ireland projects. He has published over 70 papers and actively participates in a number of technical programme committee for various conferences. Sasitharan was the TPC co-chair for ACM NANOCOM 2014 and IEEE MoNaCom 2011, both conferences which he co-founded. He is currently an editor for the IEEE Internet of Things journal and Elsevier Nano Communication Networks. His current research interests includes bio-inspired communication networks, as well as molecular communications. Sasitharan is an IEEE Senior member.

Robert Mullins Robert Mullins received his Bachelor in Computer Science and Mathematics at University College Cork, followed by Masters in Computer Science from also the University College Cork. Since joining TSSG in 2005, Robert managed the IMS ARCS Academic Consortium which focused on providing Research and Development in IMS (IP Multimedia System) technology, together with Business and Marketing Analysis to a consortium of Irish companies involved in the Telecommunications industry. Robert also has a long track record in European Research having participated in various roles in FP6 and FP7 projects including ICT Daidalos. One of Robert's most recent activities involved leading an EU commission sponsored group developing a roadmap for future research in the application of Artificial Intelligence methods to Software Engineering problems particularly in the area of the automatic adaptation and evolution of software systems and of improving and automating the software development and maintenance processes. Most recently Robert successfully coordinated the H2020 5GPPP CogNet proposal. This project is focused on next generation Autonomic Network Management systems and the application of Machine Learning algorithms to manage QoS and QoE for 5G networks and the Internet of Things.